Fifth International Conference on CFD in the Process Industries
CSIRO, Melbourne, Australia
13-15 December 2006

A THREE-DIMENSIONAL SIMULATION OF A CYCLONE DRYER

P. Bunyawanichakul[1], M. P. Kirkpatrick[2], J. E. Sargison[1], and G. J. Walker[1]

[1] University of Tasmania, Hobart, TAS 7001, AUSTRALIA
[2] University of Sydney, Sydney, NSW 2006, AUSTRALIA

ABSTRACT

The commercial computational fluid dynamics package CFX is applied to simulate the performance of a multichamber cyclone dryer used in the chemical industry. The gaseous phase is modelled using an Eulerian formulation, while the particle phase is modelled using a Lagrangian particle tracking approach. One- and two-way coupling between continuous and dispersed phases are included and turbulence is modelled using the RNG $k-\varepsilon$ turbulence model. The numerical model is validated through comparison of the predicted residence time distribution, velocity, temperature and humidity with experimental measurements taken in a laboratory scale cyclone dryer using spherical silica-gel particles. The numerical model is then used to investigate the effects of changes in various operating parameters such as the inlet air conditions, the particle feed rate and the number of chambers in the dryer.

NOMENCLATURE

C_D	drag coefficient
c_p	specific heat capacity
$D_{v\text{-}a}$	diffusivity of water vapour fraction in gas phase
d_p	particle diameter
E	exit age distribution or residence time distribution
F	mass flow rate
$\mathbf{g}$	gravitational acceralation
h	enthalpy
h_{tot}	total enthalpy
h_{fg}	latent heat of vaporisation
$\mathbf{I}$	unit tensor
k	turbulence kinetic energy
m_p	mass of particle
m_w	mass of liquid constituent in the particles
P	pressure
r	fraction of water mass in substance
S_E	energy source
$\mathbf{S_M}$	momentum source
S_{MS}	mass source
T	temperature
t	time
$\mathbf{u}$	velocity vector
V	inlet velocity
X	moisture content of particles
Y	humidity of air
Z	elevation from base of dryer inlet
ε	turbulence dissipation rate
λ	thermal conductivity
μ	effective dynamic viscosity
μ_t	turbulent dynamic viscosity
ρ	density
τ	mean residence time
Γ_t	turbulence diffusivity
NP_i	number of particles have left the computational domain at t_i
Pr_t	turbulence Prandtl number
Re	Reynolds number
Sh	Sherwood number

Subscripts

diff	differential
exp	experimental result
f	gas
p	particles
in	inlet condition
num	numerical result
out	outlet condition

INTRODUCTION

A type of swirling flow dryer known commercially as the "Cyclone dryer" has been used in the chemical processing industries since the 1980's to remove moisture from powder and granular material (Hienze, 1984). Korn (2001) has reported the drying of chemical substances with this device. It consists of a cylindrical tower containing a series of inverted conical baffles with central orifices, which divide the tower into chambers (see Fig. 1). The moist particulate matter is fed into a stream of hot, dry air, which then enters the dryer tangentially at the base of the tower, creating a rotating flow within the dryer which is considerably more complex than that seen in cyclonic separators. A precessing central vortex forms within the open region at the centre of the tower, while recirculation zones form within each of the chambers. The central vortex and through-flow jet transports the particles upwards from chamber to chamber. Most of the drying occurs within the chambers where the particles spend time trapped in the recirculating air flow. This system ensures adequate residence time and excellent mixing between the hot dry gas and the moist particles, which enables rapid transfer of moisture from the particles to the gas.

Very little performance data for this device has been published in the open literature Traditionally, because of a lack of understanding of the complex gas flow patterns and their interactions with entrained particles, dryer chambers have been designed using data correlations based on experience from existing installations and pilot plant tests. Recent advances in computational fluid dynamics (CFD) have now created the possibility of obtaining numerical predictions for these flows. Bunyawanichakul et al. (2006) reported three-dimentional numerical simulations of single-phase flow in a three-chamber cyclone dryer. Reynolds-Average Navier-Stokes (RANS) CFD simulations were performed using the commercial CFD code CFX5.7 for different mesh types, turbulence models, advection schemes, and mesh resolution to find the optimal model. Results of the

optimised simulation were compared with data from experimental model studies. Useful descriptions of the axial and tangential velocity distributions were obtained, and the pressure drop across the cyclone dryer chamber was predicted with an error of approximately 10%. The geometry of the cyclone dryer used for the experimental investigation is shown in Figure 1. It is characterised by the principal diameter D of 0.5 m, and the geometric ratios detailed in Figure 1.

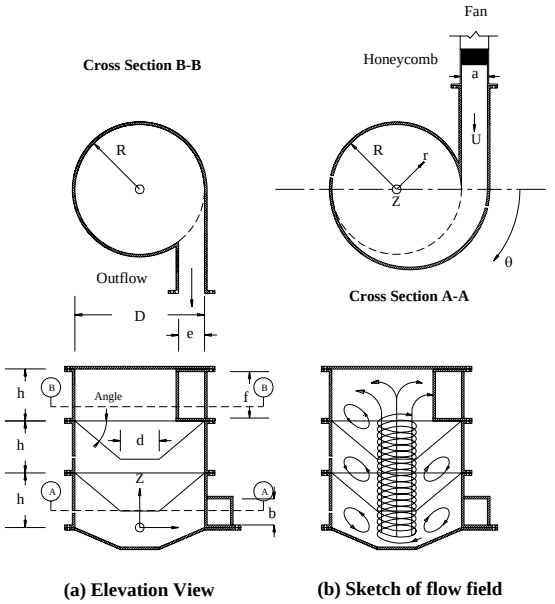

Figure 1: Schematic diagram of 3-chamber cyclone dryer geometry (a/D = b/D = e/D = 0.2; d/D = 0.3; f/D = 0.36; h/D = 0.4 Angle = 40^o)

The performance of a cyclone dryer is directly related to the changes of temperature and moisture content of air and solid particles during drying. These changes depend on both the air-flow pattern and the particle trajectories inside the drying chambers. In the present investigation the CFX 5.7 code was used to calculate both the air-flow pattern as well as particle trajectories. The optimal single-phase model (Bunyawanichakul et al. 2006) was used as an initial condition to predict the particle trajectories as well as the changes in temperature and humidity of both air and solid particles during drying, by solving the conservation of mass, momentum and energy equations based on an Eulerian/Lagrangian particle transport model.

The performance of the laboratory scale dryer was investigated experimentally using silica-gel particles as the drying material to provide the experimental data for numerical validation. Silica gel particles were chosen because they are roughly spherical and hence approximate the particle geometry assumed by the standard drag and heat and mass transfer models in CFX. The dryer configurations tested were the 3 chamber version shown in Fig. 1 and a 4 chamber arrangement in which the central chamber of Fig.1 was duplicated.

NUMERICAL MODEL DESCRIPTION

Steady state three-dimensional equations for continuity, momentum and energy were used for this study. The gas phase was modelled as a continuum and the solid phase was modelled as discrete particles. A Lagrangian/Eulerian approach was applied to model particle transport. A brief introduction of the modelling technique is given below.

Governing conservation equations for continuous phase

The equations for continuity, momentum and energy are;

$$\nabla\cdot\left(\rho_f\mathbf{u}\right)=S_{MS} \tag{1}$$

$$\nabla\cdot\left(\rho_f\mathbf{u}\otimes\mathbf{u}\right)=-\nabla P+\nabla\cdot\left(\mu\left(\nabla\mathbf{u}+(\nabla\mathbf{u})^{\mathbf{T}}\right)\right)+\left(-\rho_f\overline{\mathbf{u}'\otimes\mathbf{u}'}\right)+\mathbf{S_M} \tag{2}$$

$$\nabla\cdot\left(\rho_f\mathbf{u}h_{tot}\right)=\nabla\cdot\left(\lambda\nabla T_f\right)+\left(-\rho_f\overline{\mathbf{u}'h}\right)+S_E \tag{3}$$

where h_{tot} is the total enthalpy calculated from $h+(\mathbf{u}^2/2)$. h is enthalpy calculated from c_pT_f. The turbulent flux terms on the right hand side of equations (2) and (3) are modelled by using the eddy viscosity and diffusivity μ_t and Γ_t as shown:

$$-\rho_f\overline{\mathbf{u}'\otimes\mathbf{u}'}=\mu_t\left(\nabla\mathbf{u}+(\nabla\mathbf{u})^{\mathbf{T}}\right)-\frac{2}{3}\rho_f k\mathbf{I}-\frac{2}{3}\mu_t\nabla\cdot\mathbf{u}\mathbf{I} \tag{4}$$

$$-\rho_f\overline{\mathbf{u}'h}=\Gamma_t\nabla h \tag{5}$$

The eddy diffusivity is defined as a function of eddy viscosity by

$$\Gamma_t=\mu_t/Pr_t \tag{6}$$

and the eddy viscosity (μ_t) is obtained using the RNG $k-\varepsilon$ turbulence model, as previously validated in Bunyawanichakul et al. (2006).

Governing equations for dispersed phase

Based on the solution obtained for the continuous phase, the Lagrangian/Eulerian approach was used to calculate the particle trajectories. The governing force balance equation for the dispersed phase is the Basset, Boussinesq and Oseen equation (BBO) described in Crowe et al. (1997). Interactions between particles were neglected. One-way coupling between the particle and gas phases was applied for the particle residence time distribution (RTD) calculation, but two-way gas-particle coupling was used for all velocity field and drying simulations.The BBO equation integrates the force balance on the particle by considering only dispersed phase inertia, the aerodynamic drag force, and the gravity force. The particle sources in the fluid phase momentum equations were obtained by solving a transport equation for the sources. From the BBO equation, the equation for the momentum source is expressed as

$$\frac{\pi d_p^3\rho_p}{6}\frac{d\mathbf{u}_p}{dt}=\frac{1}{8}\pi\rho_f d_p^2C_D\left|\mathbf{u}-\mathbf{u}_p\right|\left(\mathbf{u}-\mathbf{u}_p\right)+\frac{1}{6}\pi d_p^3\left(\rho_p-\rho_f\right)\mathbf{g} \tag{7}$$

Heat and mass transfer

In general, moisture transfer between the continuous and particle phases during the constant drying rate period is assumed to satisfy the equation (ANSYS 2002)

$$\frac{dm_w}{dt}=\pi d_pD_{v-a}Sh(r_p-r_f) \tag{8}$$

where the Sherwood number is given by

$$Sh = 2 + 0.6 Re_p^{0.5} \left(\mu / D_{v-a}\right)^{1/3} \quad (9)$$

The rate of temperature change is governed by two physical processes: convective heat transfer and latent heat transfer associated with mass transfer of water. The equation of energy balance is given by

$$m_p c_p \frac{dT_p}{dt} = \pi d_p \lambda_p Nu (T_f - T_p) + h_{fg} \frac{dm_w}{dt} \quad (10)$$

The Nusselt number is calculated from

$$Nu = 2 + 0.6 Re_p^{0.5} \left(\mu c_p / \lambda\right)^{1/3} \quad (11)$$

where Re_p is particle Reynolds number calculated from

$$Re_p = \rho_f \left(\mathbf{u} - \mathbf{u_p}\right) d_p / \mu_f \quad (12)$$

Numerical model set up

The simulations presented in this paper were performed using CFX 5.7. The structured mesh employed was generated using ICEM 5. As discussed in Bunyawanichakul et al. (2006), reasonable accuracy of mean-flow prediction and computational time were obtained using the RNG $k-\varepsilon$ turbulence model with second-order accurate differencing scheme and 58,780 elements. Parcels of the particulate phase were tracked using the Lagrangian particle-tracking feature of CFX 5.7 and a turbulence dispersion model.

The fact that the RNG $k-\varepsilon$ model gave better agreement with the experiment results than a Reynolds Stress Model for this problem is contrary to the finding of the other reserachers who have modelled cyclone devices. We believe that this may be due to the fact that we have performed steady-state simulations rather than unsteady simulations. The precessing central vortex that occurs within the cyclone dryer constitutes a larger scale unsteady feature that cannot be parameterised by the turbulence model. It is likethat runnung a steady state simulation of what is essentially an unsteady flow could lead to unpredictable behaviour of the turbulence models.

The mean diameter of the silica gel particles was 3.25 mm. In the simulations presented in this paper a restitution coefficient was used to determine the behaviour of particles impacting at the wall of the cyclone dryer. The particles were allowed to rebound elastically from the wall, which means the restitution coefficient was set to unity. Particle agglomeration was neglected within the dryer. These assumptions have been used by many researchers for cyclone separator simulations (e.g. Griffiths 1996; Correa 2004 a&b).

The first series of simulations was performed using one-way coupling to simulate the residence time distribution of particles. Simulations using silica gel particles were run with feed rates of 0.034, 0.0576, and 0.0778 kg/s and inlet air velocities of 23, 21 and 19 m/s for three- and four-chamber cyclone dryer configurations. These feed rates and inlet air velocities were the same as those used experimentally. The number of particles leaving the computational domain each time interval were counted and used to calculate the exit age distribution or residence time distribution E (t) following the method described in Madhiyanon (2001). Simulation results of first series were compared with the experimental RTD obtained by the stimulus-response technique using tracer injection (Levinspiel 1972).

A second series of simulations was using two-way coupling conducted by setting up the inlet air and particle mass flow rates, temperature, and moisture content according to the experimental tests in Bunyawanichakul (2006). The evaporation of water in the particles was simulated by employing the evaporation model incorporated within CFX 5.7, which models heat and mass transfer between the discrete and gas phases as described above. The parameters of those simulations are shown in Table 1 for three-and four chamber cyclone dryers.

CFD Run	F_p	$T_{p,in}$	X_{in}	F_f	$T_{f,in}$	Y_{in}
	kg/s	°C	kg/kg	kg/s	°C	kg/kg
Three-chamber configuration						
1	0.0585	19.7	0.266	0.243	57.8	0.00659
2	0.0256	19.7	0.231	0.252	57.4	0.00773
3	0.0256	21.6	0.229	0.239	68.9	0.00854
4	0.0256	20.8	0.232	0.234	81.2	0.00783
5	-	-	-	0.252	57.4	0.00773
6	0.0433	19.7	0.231	0.252	57.4	0.00773
7	0.0585	19.7	0.231	0.252	57.4	0.00773
8	0.0256	19.7	0.231	0.252	68.9	0.00773
9	0.0256	19.7	0.231	0.252	81.2	0.00773
10	0.0256	19.7	0.210	0.252	57.4	0.00773
11	0.0256	19.7	0.400	0.252	57.4	0.00773
Four-chamber configuration						
12	0.0433	22.0	0.233	0.220	58.7	0.00816
13	0.0256	21.9	0.181	0.229	59.8	0.00699
14	0.0256	22.0	0.186	0.224	68.9	0.00711
15	0.0256	22.2	0.187	0.212	81.5	0.00656
16	-	-	-	0.229	59.8	0.00699
17	0.0433	21.9	0.181	0.229	59.8	0.00699
18	0.0585	21.9	0.181	0.229	59.8	0.00699
19	0.0256	21.9	0.181	0.229	68.9	0.00699
20	0.0256	21.9	0.181	0.229	81.5	0.00699
21	0.0256	21.9	0.233	0.229	59.8	0.00699
22	0.0256	21.9	0.400	0.229	59.8	0.00699

Table 1: Modelling conditions of silica gel drying

SIMULATION RESULTS AND VALIDATION

RTD simulation

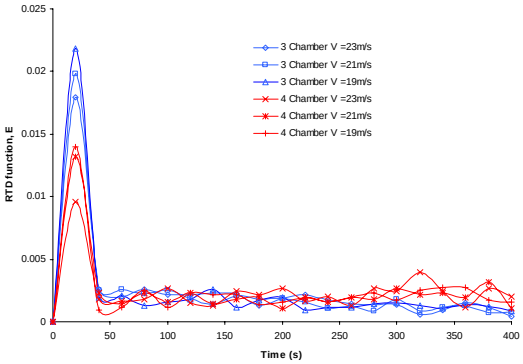

Figure 2: Numerical RTD curves of silica-gel particles

Figure 2 shows the residence time distributions for silica-gel particles at different inlet air velocities for three- and four-chamber cyclone dryers obtained from the simulation results. These curves were calculated using the method

discussed previously. The residence time distribution profiles exhibit an abrupt peak followed by a long tail. The peak height increases when the number of chambers is decreased, while the effect of increasing inlet air velocity is to reduce peak height for both three- and four-chamber dryers. The curves are independent of particle feed rate because of the one-way gas-particle coupling applied for the RTD simulation.
Table 2 compares the mean residence time obtained from the experimental data with the simulation results. The mean residence time from the simulations increased with the number of cyclone dryer chambers, while changing this parameter had little effect on the experimental results. Varying and inconsistent trends of mean residence time for both experimental and numerical results were obtained when the inlet air velocity was changed.

Comparisons of numerical and experimental residence time distributions (RTD) for silica gel particles in a three-chamber cyclone dryer are shown in Figures 3. The model prediction shows a significantly higher peak value, but the tails of both curves correspond fairly closely. This trend was also observed for four-chamber cyclone dryer simulations (Bunyawanichakul 2006).

Case	Number of chamber	$v_{f,in}$ m/s	F_p kg/s	τ_{exp} s	τ_{num} s
1	3	19	0.0778	134	122
2	3	21	0.0778	132	119
3	3	23	0.0778	148	126
4	4	19	0.0778	136	173
5	4	21	0.0778	138	171
6	4	23	0.0778	132	189

Table 2: Comparison of experimental and numerical mean particle residence times

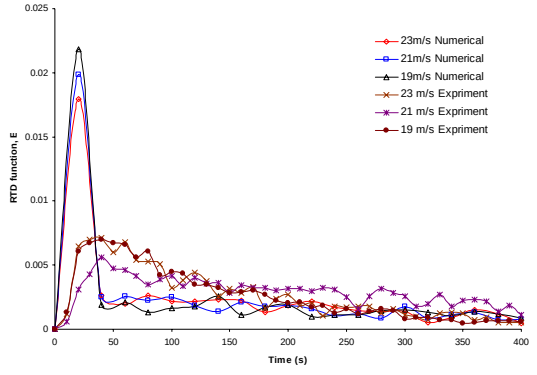

Figure 3: Experimental and numerical RTDs for silica gel particles at inlet air velocity of 19, 21 and 23 m/s for three-chamber cyclone dryer

The differences between the residence time distribution curves at early times indicate that a significant number of particles are leaving the cyclone chamber faster than expected in the numerical simulation. These deviations may be mainly attributed to two factors:

(a) the experimental mean residence time was found to be strongly dependent on particle feed rate, as shown in Bunyawanichakul (2006). This fact was not taken into account in the Lagrangian particle transport modelling, which neglected interactions between particles and the influence of the particle phase on the gas phase;

(b) as discussed in Bunyawanichakul et al. (2006), although the simulated velocity distributions were similar to the experimental data near the central core, there was significant deviation in the outer region due to the diffusive nature of the RNG $k-\varepsilon$ turbulence model. Differences in the fluid phase velocity distribution will influence the particle residence time. More importantly, the excessive diffusion predicted by the turbulence model will lead to an overprediction of the drag force acting on the particles, and a resulting underprediction of the residence time.

In summary, the simulated residence time distributions deviate significantly from the experimental data. However, the quantitative results for mean residence time are of the same order of magnitude.

Drying simulation

Figure 4 (a) shows the tangential velocity distributions produced at different silica gel particle feed rates, inlet air temperatures, and initial particle moisture content, respectively. The predicted tangential velocity decreases when the silica gel feed rate increases. The presence of the particulate phase has a great influence on the gas tangential velocity distribution, but the change in the gas axial velocity is negligible in comparison. The effect of different inlet air temperatures is shown in Figure 4 (b). Changing the inlet air temperature causes only small changes in the tangential velocity distribution. The tangential velocity is not significantly altered by changing initial moisture content of the silica gel. Similar results were obtained for the tangential velocity distribution in the four-chamber cyclone dryer configuration.

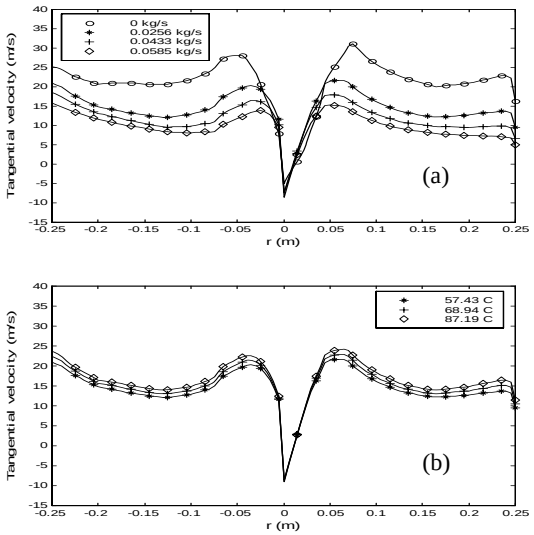

Figure 4: Predicted tangential velocity distribution in 3-chamber dryer at 0.055 m elevation at different: (a) particle feed rates; (b) inlet air temperature

Figures 5 (a) and 7 (a) show the predicted temperature distributions in the first and second chambers of a three-chamber cyclone dryer at different silica gel feed rates. The corresponding humidity distributions are depicted in Figures 6 (a) and 8 (a). Figures 5 (a) and 6 (a), indicate that the first part of the drying takes place in the fast flowing core of the first chamber, where the air

temperature decreases and humidity increases. The second part of the drying process takes place in the outer region of the second chamber where the air temperature further decreases and humidity increases as shown in Figures 7 (a) and 8 (a). These phenomena can be explained by most of the particles being trapped in the outer region of the intermediate chamber for a long time. Drying takes place in this region at a high particle concentration, which encourages a high intensity of particle and gas mixing. This pattern of temperature and humidity distributions was also obtained for four-chamber cyclone dryers.

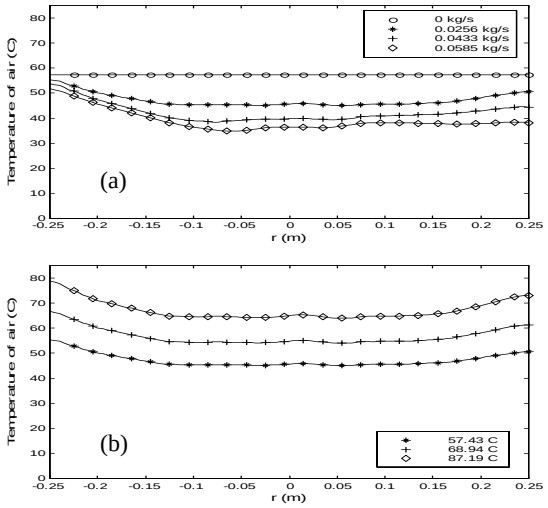

Figure 5: Predicted air temperature distribution in 3-chamber dryer at 0.055 m elevation at different: (a) particle feed rates; (b) inlet air temperature

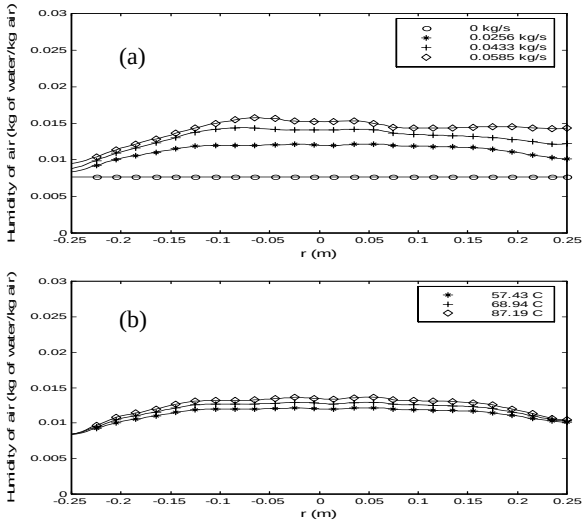

Figure 6: Predicted humidity distribution of air in 3-chamber dryer at 0.055 m elevation at different: (a) particle feed rates; (b) inlet air temperature

The predicted effects of inlet air temperature on the distributions of air temperature and humidity are shown in Figures 5&7 (b) and 6&8 (b), respectively. It was found that the air temperature distributions remained similar in shape and were shifted by an almost constant differential throughout the chamber. Significant differences in the air humidity distributions were also observed. A higher inlet air temperature gives a higher driving force for water evaporation, and therefore the air humidity increases when the inlet air temperature increases as shown in Figures 6 (b) and 8 (b) for the first and second chamber. A higher water evaporation was predicted in the central region of first chamber and outer region of the second chamber, where particles were trapped by the flow recirculation.

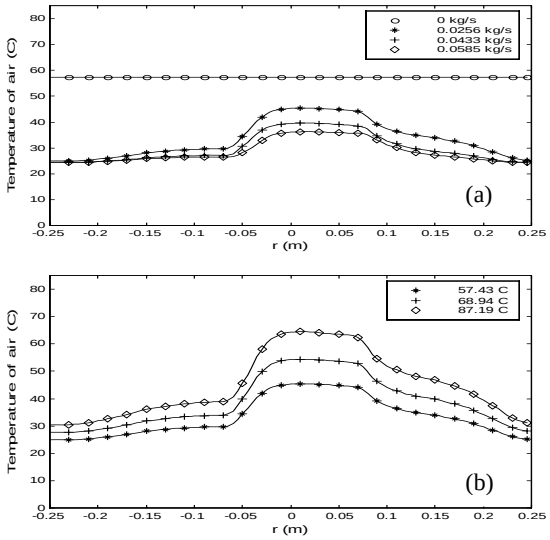

Figure 7: Predicted air temperature distribution in 3-chamber dryer at 0.255 m elevation at different: (a) particle feed rates; (b) inlet air temperature

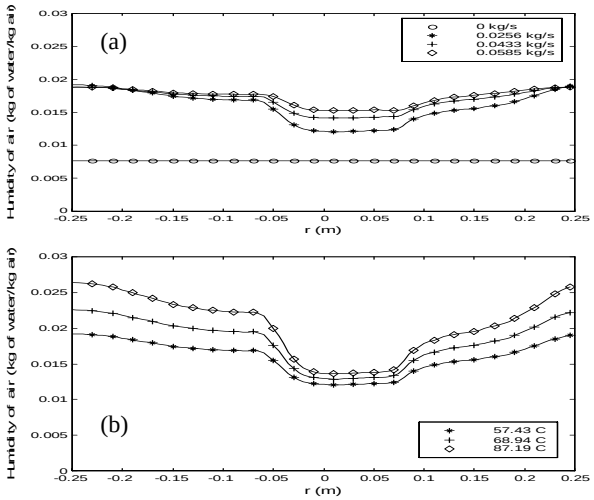

Figure 8: Predicted humidity distribution of air in 3-chamber dryer at 0.255 m elevation at different: (a) particle feed rates; (b) inlet air temperature

On the other hand, there was little difference in the humidity and temperature of the air for different initial moisture contents of silica gel particles. Similar trends were predicted for the humidity and air temperature distributions in a four-chamber cyclone dryer.

Table 3 compares the numerical and experimental results for drying of silica gel particles in three- and four-chamber cyclone dryers. The numerically predicted humidity difference of the air between inlet and outlet is somewhat higher than the measured value. However the numerically

predicted air temperature differential is lower than the measured value. This indicates that the heat and mass transfer model used in this study overpredicts the mass and energy transfer rates.

CFD run	$\Delta T=T_{f,in}-T_{f,out}$, °C			$\Delta Y=Y_{out}-Y_{in}$, kg/kg		
	$(\Delta T)_{exp}$	$(\Delta T)_{num}$	$(\Delta T)_{diff}$	$(\Delta Y)_{exp}$	$(\Delta Y)_{num}$	$(\Delta Y)_{diff}$
1	17.26	22.61	5.35	0.0061	0.0078	0.0017
2	11.42	16.71	5.29	0.0042	0.0058	0.0016
3	16.26	22.16	5.90	0.0059	0.0075	0.0016
4	20.39	31.43	11.0	0.0082	0.0102	0.0020
12	15.54	24.03	8.49	0.0048	0.0082	0.0034
13	32.58	40.90	8.32	0.0072	0.0106	0.0034
14	16.71	23.76	7.05	0.0050	0.0085	0.0035
15	12.21	19.94	7.73	0.0032	0.0068	0.0036

Table 3: Comparison of experimental and numerical air humidity and temperature at cyclone dryer outlet. Run numbers as in Table 1.

The model employed to simulate heat and mass transfer between the particles and air is based on the concept of droplet evaporation, which assumes that the vapour at the surface of the particles is always saturated. This model does not accurately calculate the heat and mass transfer during the falling rate drying period in which the rate of water evaporation is controlled by moisture diffusion inside the particle. This is believed to be a more accurate description of the drying process of silica gel particles.

While the numerical model gives quite reasonable trends for changes in the humidity and temperature, the quantitative accuracy of the predicted overall differentials in temperature and humidity is only fair. Larger deviations were obtained for a dryer with a higher number of chambers, as seen by comparing the results for the four-chamber configuration (runs 12, 13, 14 and 15) with the results for three-chamber configurations (runs 1, 2, 3, and 4).

CONCLUSIONS

Three-dimensional numerical simulations of particle transport coupled with heat and mass transfer inside a cyclone dryer have been carried out using CFX 5.7, a RANS-based commercial CFD code. The optimal single-phase steady state model based on a RNG k-ε turbulence model with hexahedral mesh using a second-order accurate advection scheme (Bunyawanichakul et al. 2006) was used for the fluid phase. A Lagrangian particle transport model was added to calculate particle trajectories as well as the changes in temperature and humidity of both air and solid particles during drying.

Initial calculations used one-way coupling in CFX 5.7 to determine the particle residence time distribution inside the cyclone dryer. The RTD curves changed with inlet air velocity, but were not significantly influenced by particle feed rates. This was due to the one-way coupling failing to properly account for particle-particle and particle-fluid interactions. While the magnitude of the mean residence time was correctly predicted, the variation of calculated mean residence time with inlet velocity was not always consistent with the experimental observations.

Some experimental tests of silica gel particle drying were also simulated to assess the performance of CFX5.7 for predicting drying rates. In this case, two-way coupling was used, taking into account mass, momentum and energy transfer between the particle and gas phases. These simulation results indicated the parameter with most influence on the tangential velocity distribution to be the particle feed rate, while the inlet air temperature had the most influence on the temperature and humidity distributions. Significant errors were observed in the predicted overall differentials in air temperature and humidity between inlet and outlet of the cyclone dryer. The model used here overpredicted both the mass and energy transfer, giving errors up to 50% in temperature differential and 100% in humidity differential.

ACKNOWLEDGMENTS

The support of School of Engineering, University of Tasmania for the cyclone dryer prototype fabrication and ANSYS Inc. for the CFX academic software licence is gratefully acknowledged. The first author expresses his gratitude to Srinakarinwirot University, Thailand for financial support during his PhD study at the University of Tasmania.

REFERENCES

ANSYS, (2002), " Turbulence wall function theory and initial condition modelling", *CFX5 solver theory*, ANSYS Canada Ltd., Waterloo, Canada.

BUNYAWANICHAKUL, P., (2006), " Development of a cyclone rice dryer", Ph.D. Thesis, University of Tasmania, Tasmania, Australia.

BUNYAWANICHAKUL, P., KIRKPATRICK, M., SARGISON, J.E., and WALKER, G.J., (2006), " Numerical and experimental studies of the flow field in a cyclone dryer", *ASME Journal of Fluid Engineer.* (In Press).

CORREA, J.G.L., GRAMINHO, D.R., SILVA, M.A. and NEBRA, S.A., (2004a), "Cyclone as a sugar cane bagasse dryer", *Chinese Journal of Chemical Engineering*, **12**, 826-830.

CORREA, J.G.L., GRAMINHO, D.R., SILVA, M.A. and NEBRA, S.A., (2004b), "The cyclone dryer - a numerical and experimental analysis of the influence of geometry on average particle residence time", *Brazilian Journal of Chemical Engineering*, **21**, 103-112.

CROWE, C., SOMMERFIELD, M., and TSUIJI, Y., (1997), "Multiphase flows with droplets and particles", CRC Press, New York.

GRIFFITHS, W.D. and BOYSAN, F., (1996), "Computational fluid dynamics (CFD) and empirical modeling of the performance of a number of cyclone samples", *J. Aerosol Sci.*, **27**, 281-304.

HEINZE, C., (1984), "New cyclone dryer for solid particles", *Ger.Chem.Eng.*,**7**, 274-279.

KORN, O., (2001), "Cyclone dryer: A pneumatic dryer withincreased solid residence time", *Drying Technology*, **19**, 1925-1937.

LEVENSPIEL, O., (1972), "Chemical reaction engineering", John Wiley&Sons, New York, USA.

MEDHIYANON, T., (2001), "Drying of grains by spouted bed technique", Ph.D. Thesis, King Mongkut University of Technology (Thonburi), Bangkok, Thailand.